Noise and Transit Time in Ungated FET Structures

Javier Mateos, Tomás González, Daniel Pardo, Patrick Tadyszak, François Danneville, and Alain Cappy

***Abstract*—Using a classical Monte-Carlo simulation, tested by means of the comparison with experimental measurements of $I-V$ characteristics and noise temperature, we compare the frequency and noise behavior of GaAs/$Al_{0.2}Ga_{0.8}As$ ungated HEMT (called u-HEMT) with respect to GaAs ungated MESFET (u-MESFET). The small fraction of Al in the AlGaAs makes the real-space transfer between the GaAs and AlGaAs layers become important; its effects will be analyzed. As main tool for the comparison we employ the transit time of the electrons through the devices. This magnitude can give exact information not only about the speed but also about the noise behavior of the devices. We have observed an important reduction of the switch-on time which passes from 14 ps in the u-MESFET to 10 ps in the u-HEMT (at a biasing of 2.0 V). The transit-time distribution shows that the current in the u-HEMT comes from electrons whose velocities do not spread as much as in the u-MESFET, where the distribution is wider. This leads to a lower value of the current variance, which is related to the total noise spectrum of the devices.**

I. Introduction

In THE PAST, high electron mobility transistors (HEMT's) have received increasing interest because of their suitability for high-speed, high-power, and low-noise applications. This behavior is accomplished by using the energy barrier created by a heterojunction to restrict the current to flow through a low-doped material. In this way, the amount of impurity scattering which conduction electrons undergo is reduced considerably, thus reaching higher velocity and giving rise to higher current and lower fluctuations.

The most widely used HEMT's are made using the GaAs/$Al_xGa_{1-x}As$ material system, which exhibits a much better frequency and noise performance than the usual GaAs MESFET. But the Al mole fraction must not exceed 20%, because problems such as persistent photoconductivity [1], [2] and drain collapse [3] arise due to the presence of DX centers. Thus in the fabrication of our u-HEMT's we will use an Al mole fraction of 20%. At this small Al concentration the conduction band edge discontinuity is quite narrow, and so the real-space transfer (RST) effects become very important. These effects reduce the confinement of electrons in the GaAs channel, therefore deteriorating the overall characteristics.

Manuscript received September 13, 1996; revised March 25, 1997. The review of this paper was arranged by Editor J. Xu. This work was supported in part by the EC program ELEN through Contract ERBCHRXCT 920047, and Project TIC95-0652 from the Comisión Interministerial de Ciencia y Tecnología (CICYT).

J. Mateos, T. González, and D. Pardo are with the Departamento de Física Aplicada, Universidad de Salamanca, Salamanca 37008, Spain.

P. Tadyszak, F. Danneville, and A. Cappy are with the Département Hyperfréquences et Semiconducteurs, Institut d'Electronique et Microélectronique du Nord U.M.R. C.N.R.S. no. 9929, Villeneuve D'Ascq Cédex 59652, France.

Publisher Item Identifier S 0018-9383(97)08283-X.

In the study of these complicated devices the Monte-Carlo particle method [4], [5] appears as a useful way to understand its macroscopic behavior by investigating the microscopic processes taking place. The values of all the interesting physical quantities in every point of the structure can be obtained, which is specially interesting near the heterojunction, where the electron concentration, energy, velocity, valley occupation, and current can make clear what is happening inside the device. Moreover, the fluctuations of the current are included without any further assumption, thus allowing the complete analysis of the noise behavior of the devices.

To reduce the complexity of usual two ports devices a HEMT without gate will be considered, but with a recessed geometry. One ungated recessed HEMT has been fabricated, its static and noise characteristics have been measured, and reproduced with the Monte-Carlo simulation.

The GaAs/AlGaAs heterojunction produces an accumulation layer in the GaAs, where quantum effects become important in electron transport, with the presence of a two-dimensional electron gas (2-DEG). In previous works these effects have already been introduced in the Monte-Carlo simulation in different degrees of approximation [6]–[8]. We will neglect all the quantum effects, which has been demonstrated to be a good approximation to characterize the electron dynamics inside the device [9]–[12]. Experimental results of both static characteristics and noise temperature agree with the simulation, this fact confirms the validity of the modeling used for these heterojunction devices.

This work will study the influence of the heterojunction and particularly the effects of RST on speed and noise behavior, through the comparison of an u-HEMT and an u-MESFET. To realize this, an u-MESFET with similar $I-V$ characteristics is simulated (the model has already been explained and tested with experimental data [13]). The analysis of the time the electrons take to pass through the device (transit time) is a good instrument not only to show the speed, but also to have an estimation of the noise behavior. Firstly, the average value of the transit time coincides with the switch-on time of usual two-ports devices [14], so giving a good measure of how fast the device is. And secondly, if we focus on the distribution of the transit time of electrons we can get an idea of the diffusion noise of the device, since it shows how the velocities of the carriers spread.

In Section II the fabricated and simulated structures will be shown. The details of the Monte-Carlo simulation will be discussed in Section III. The main results will be presented in Section IV, and finally Section V summarizes the principal conclusions of our work.

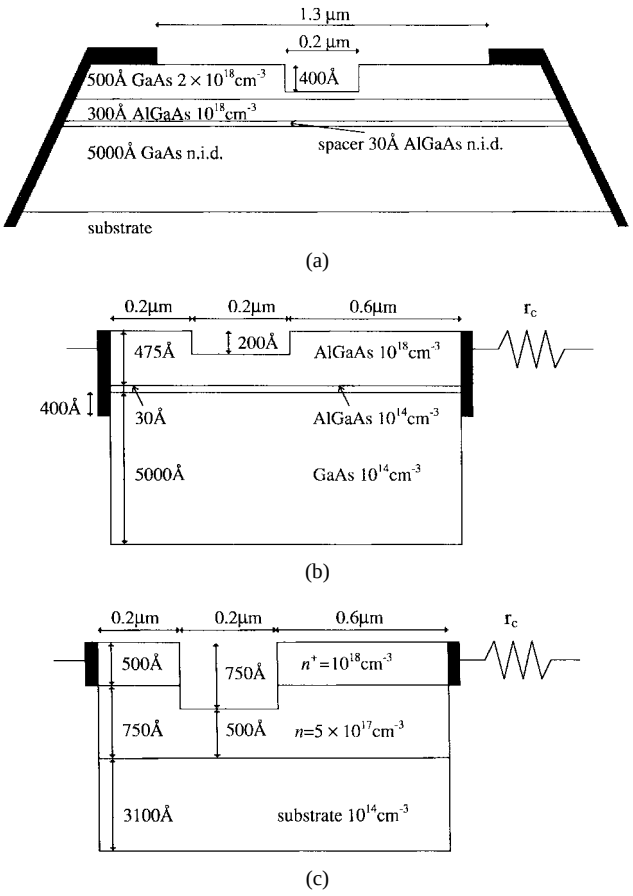

Fig. 1. Schemes of: (a) fabricated u-HEMT, (b) simulated u-HEMT, and (c) simulated u-MESFET.

II. Real and Simulated Structures

Schematic drawings of the real and simulated structures are shown in Fig. 1. We have used ungated devices to diminish the complexity and to reduce the number of parameters to be calculated (mainly when dealing with noise), but maintaining the recessed geometry. This kind of geometry, together with the effects of the surface potential [13], produces high fields and hot electrons in the channel, two interesting effects to be studied. Fig. 1(a) presents the real u-HEMT, and Fig. 1(b) the simulated one. We can notice some differences. The GaAs top layer is not included in the simulation since it is used to realize the ohmic contacts and it does not modifies the conduction through the device, so the thickness of the AlGaAs layer has been increased in the simulation to reproduce the behavior of the two cap layers. The series resistance r_C represents the contact resistance and the effect of the nonsimulated ohmic parts of the device (like part of the region between the source and the recess). The effect of the plasma etching used to make the recess can deteriorate the properties of the material, and so the depth of the recess of the simulated structures is taken as an adjustable parameter. These differences in the geometry come from the attempt to optimize the simulation time, and to adjust the values of the calculated current. The details concerning of all these modifications in the simulated device are widely explained in [13].

In Fig. 1(c) the simulated u-MESFET is shown. The length of the device is the same as in the u-HEMT. The depth of the recess has been adjusted to obtain an $I-V$ characteristic similar to that of the u-HEMT. In this way, in the following we will compare the behavior of a u-HEMT and a u-MESFET with the same source-drain distance and analogous static performance.

III. Monte-Carlo Simulation

The simulation have been performed using an ensemble Monte-Carlo self-consistently coupled with a 2-D Poisson solver. The effect of a series resistance and a surface potential in the three walls of the recess have been included; the details have been given elsewhere [13], [15], [16]. The value of the series resistance is 5×10^{-4} Ωm. The Pauli exclusion principle is considered using the rejection technique described in [17]. The devices are divided into rectangular cells whose dimensions are: 50 Å in the direction of the current and ranging from 10 Å to 50 Å in the transversal direction (in the accumulation layer near the heterojunction it is necessary to have more precision). The Poisson solver uses a direct matrix method (LU decomposition), suitable for non uniform meshes and complicated geometries. Ohmic boundary conditions are considered at the contacts, so the number of carriers inside the device is adjusted automatically [18]. The number of simulated particles ranges from 13 500 to 15 500 depending on the structure and the bias point. The simulation is performed during 0.1 ns divided into time steps of 1 fs each, short enough to get a correct solution of the electric field. The scattering mechanisms taken into account are the following: ionized impurities, polar optical, both assumed as anisotropic; nonpolar optical, acoustic, and intervalley (equivalent and nonequivalent), all of which are considered isotropic. The material parameters of the three valley model (Γ, L and X) used for GaAs have been detailed in previous papers [19], [20]. The scattering mechanisms present in the $Al_{0.2}Ga_{0.8}As$ are the same than in GaAs (alloy scattering is neglected due to its weak influence). The material parameters for the $Al_{0.2}Ga_{0.8}As$ are summarized in Table I and have been obtained from several references [12], [21]–[25], choosing the values the best adapted to the parameters taken for the GaAs. The value of the conduction-band-edge discontinuity at the heterojunction is 0.145 eV [26].

In the electrodes Dirichlet conditions are assigned (the value of the potential is fixed), in the recess a constant surface charge is taken as boundary condition (the normal electric field is fixed to a constant value) and in the rest of the boundaries von Neumann conditions are given (normal electric field equal to zero) [13]. The electrodes are placed vertically extending across the heterointerface. The values of the potential assigned to these electrodes are calculated from the distribution that would appear inside the structure if real top electrodes were used [27]. This distribution has been calculated from a separated simulation at equilibrium and it is applied for every biasing. This may not be completely correct, since the distribution of the potential in the drain electrode changes with the biasing, but we have confirmed that the perturbation produced in the potential does not enter more than five meshes inside the device.

TABLE I
PHYSICAL PARAMETERS OF $Al_{0.2}Ga_{0.8}As$

Parameter	Value		
Density (Kg/m^3)	5008.0		
Sound velocity (m/s)	5240.0		
Static dielectric constant	10.46		
Optical dielectric constant	12.32		
LO Phonon energy (eV)	0.0378		
	Γ	L	X
Effective mass (m^*/m_0)	0.080	0.222	0.546
Nonparabolicity (eV^{-1})	0.56	0.48	0.30
Energy level from Γ (eV)	0.00	0.23	0.31
Number of equivalent valleys	1	4	3
Acoustic deformation potential (eV)	5.0	5.0	5.0
Optical deformation potential (10^{10} eV/m)	0.0	3.0	0.0
Optical phonon energy (eV)	0.0	0.0343	0.0
Intervalley deformation potential (10^{10} eV/m)			
from Γ	0.0	10.0	10.0
from L	10.0	10.0	5.0
from X	10.0	5.0	7.0
Intervalley phonon energy (eV)			
from Γ	0.0	0.0297	0.0313
from L	0.0297	0.0297	0.0313
from X	0.0313	0.0313	0.0313

Ohmic electrodes impose a predetermined concentration of electrons in the meshes close to them. Usually this concentration equals the doping to keep charge neutrality, which is the common condition of equilibrium. But in the heterointerface the equilibrium is reached with concentrations far from the values of the doping: in the GaAs an accumulation layer is created and in the AlGaAs a depletion of electrons appears. In our model the ohmic contact will force the concentration in the depletion region to equal the value it would exist at equilibrium (calculated previously in the same way that the potential profile).

In the accumulation layer the electrons suffer quantization of their energy, thus constituting a 2-DEG. To take into account this quantum behavior it would be necessary to solve the Schrödinger equation self-consistently with Poisson equation, and then calculate the sub-bands energy levels and the 2-D scattering rates for electrons. We will make the simulation at a semiclassical level, considering bulk band structure and scattering rates and without any quantum effect. This assumption does not introduce a significant error, as confirmed elsewhere [9]–[12], mainly when the field is high, as it occurs in the channel of our structures.

Using the classical laws of conservation of total energy and momentum perpendicular to the heterojunction, the final state when one electron moves between the GaAs and the AlGaAs (RST) is obtained. If the energy is enough to jump over the barrier, the carrier has a transmission coefficient of 1, in other case it is specularly reflected; quantum reflection and tunneling are not considered. In this kind of processes it is assumed that the electron does not change of valley, since the important variation of momentum which implies an intervalley transition makes it highly improbable [23].

Due to the stochastic nature of the Monte-Carlo method some uncertainty is present in the results, which can be estimated to be within 5% for first order quantities (current and average transit times and velocities) and 15% for second order calculations (current variance, current spectral density). It is even higher (about 20%) in the case of the noise temperature due to the additional uncertainty in the calculation of the differential resistance of the device [13].

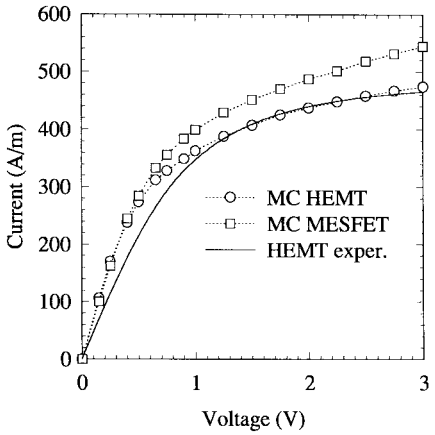

Fig. 2. $I-V$ characteristics of the real (experimental) and simulated u-HEMT's and of the simulated u-MESFET.

IV. RESULTS

Taking as a basis the $I-V$ characteristics obtained for the real u-HEMT, we have adjusted the depth of the recess in both the simulated u-HEMT and u-MESFET to obtain similar characteristics, which are presented in Fig. 2. The technological uncertainty about the plasma etching leads us to modify this parameter to achieve a similar static response. The differences in the range of low biasing can be associated to a higher resistance of the contacts, or to parasitic effects coming from the degradation of the transport properties of the channel caused by the etching.

Once the $I-V$ curve is well reproduced we try to compare the results obtained for the noise temperature. The high-frequency (2–4 GHz) noise measurement technique was detailed in [28]; in this case is simplified because of the use of one-port devices. In a previous paper we obtained a quite good agreement between simulated and measured values of this parameter in the case of the u-MESFET [13]. The noise temperature obtained for the real and simulated u-HEMT are shown in Fig. 3, together to the simulated values for the u-MESFET. It can be observed the agreement is very good in the case of the u-HEMT. This result validates the model used in our calculations, since second order quantities (as is the case of noise) are very sensitive to the device modeling. The noise temperature in the u-MESFET shows a similar dependence on the current, but taking lower values. This behavior has been confirmed by experimental measurements of similar structures with 0.15 μm of recess length.

It is a consequence of the dual origin of the noise temperature (T_n)

$$T_n = \frac{S_I r}{4K_B}. \tag{1}$$

On the one hand it reflects the noise in the output current through the spectral density of the current fluctuations (S_I),

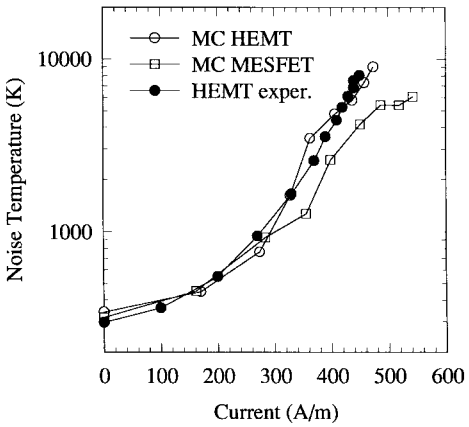

Fig. 3. Noise temperature as a function of the current of the real (experimental) and simulated u-HEMT's and of the simulated u-MESFET.

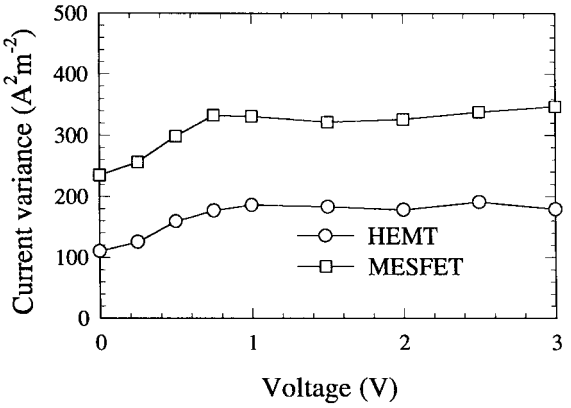

Fig. 4. Current variance of the simulated u-HEMT and u-MESFET as a function of the applied voltage.

and on the other hand it includes the small signal dynamic behavior of the device through the incremental resistance (r). K_B is the Boltzmann constant. In our case, the higher resistance of the u-HEMT in saturation (Fig. 2) leads to a higher value of the noise temperature since they have similar values of spectral density between 2–4 GHz. Thus, even if the noise temperature allows to compare the noise behavior of structures with different resistance and level of current, it does not give a clear and direct information about the current noise, since it is masked in part by the dynamic response of the devices.

The current variance represents the mean value of the squared fluctuations of the current. It is related to the whole noise spectrum and not only to a fixed frequency as it occurs for the noise temperature: moreover this magnitude is independent of the resistance. In Fig. 4 the variance of the current in the u-HEMT and the u-MESFET is plotted as a function of the voltage. It is observed that its value in the u-MESFET is much higher than in the u-HEMT (in a factor two). This difference is mainly related to the very high frequency range of the noise spectrum (THz range), which in the MESFET is quite important due to the higher doping of the conduction layer [29]. Although we can not obtain any practical information from the current variance, from a physical point of view it provides more information about the noise in the device than the noise temperature (though this is the only measurable noise parameter). Even if the absolute value of the current variance is very influenced by the very high frequency current fluctuations, its behavior as a function of the biasing is mainly determined by the effects taking place at lower frequencies (up to some hundreds of GHz). Hence, it is possible to relate these effects to the transit time distribution of the electrons.

For a better understanding of the u-HEMT performance, Fig. 5 shows the sheet carrier concentration in the GaAs accumulation layer, together with the RST current [13] flowing through the heterointerface (considered positive when the electrons go from GaAs to AlGaAs) for different biasing conditions. The sheet concentration has been calculated by integrating (summing) all the carriers present in the GaAs layer. Fig. 5(a) reveals that the effect of the surface potential reaches the accumulation layer, producing a decrease of the electron concentration in the region under the recess. If a voltage of 0.25 V is applied, the electrons flow toward the drain, but their energy is not enough to surmount the barrier of the heterojunction, so leading to a higher concentration than at equilibrium conditions in the region between the recess and the drain. When the biasing is higher, even if the electrons are more strongly injected in the GaAs layer, RST appear [as can be observed in Fig. 5(b)], making the electrons go back to the AlGaAs and decreasing the presence of carriers in the accumulation layer. When the biasing exceeds 1.0 V an accumulation domain of carriers appears in the last part of the recess due to the heating of the electrons, which pass to the higher valleys and, consequently, their velocity decrease. The increase of the sheet carrier density comes also in part from the deeper penetration of the carriers injected into the GaAs. This accumulation disappears after a short distance due to the RST, which is much easier in the L and X valleys, where the barrier imposed by the heterojunction is quite small. In Fig. 5(b) it can be observed how RST increases at the right side of the recess with the heating of electrons. The higher the biasing is, the faster the electrons heat, the accumulation forms and RST begins.

The effect of transverse domain, already reported in [30], is also detected Fig. 5(b). When the voltage is 3.0 V, the current flowing through the heterojunction changes its sign, coming from the AlGaAs to the GaAs, thus contributing to enlarge the accumulation domain ('transverse' domain because it is formed from a current perpendicular to the main flow). The transverse domain effect is less pronounced than in conventional HEMT's, where the electric field between the gate and the drain is more important. In our device the drop of the potential is more gradual. The high field effects are smoothed and arise for a higher applied voltage. This can be observed in Fig. 6, where the equipotential lines of the u-HEMT and u-MESFET under a total biasing of 2.0 V are shown. The absence of the gate terminal fixing the potential at the recess makes possible a potential drop not completely localized at the drain side of the recess, but more uniformly distributed along the whole channel. This effect is more noticeable in the u-HEMT, where an important electric field penetrates into the drain region, while in the u-MESFET

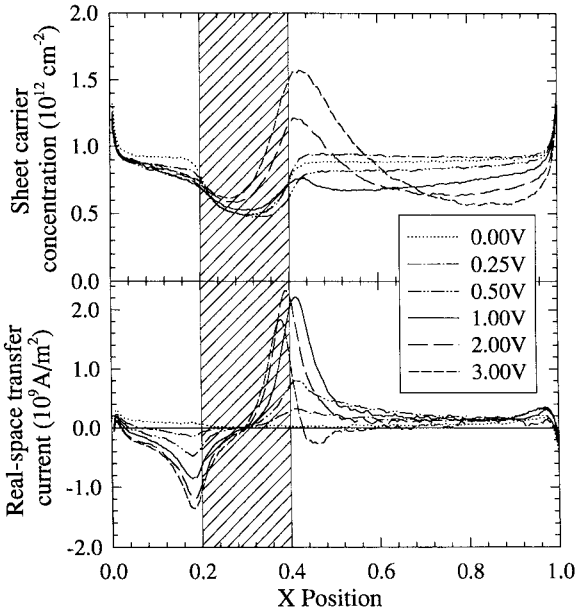

Fig. 5. (a) Sheet carrier concentration and (b) real space transfer current in the simulated u-HEMT for different biasings as a function of the position. The region under the recess is indicated by the shaded area.

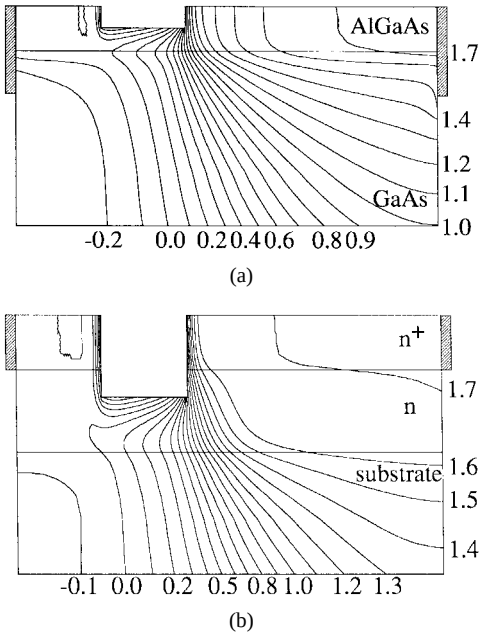

Fig. 6. Potential distribution in (a) the simulated u-HEMT and (b) u-MESFET for a biasing of 2.0 V. Only the top part of the devices is represented.

it is practically null at a short distance from the recess.

To observe how the importance of RST increases with the biasing, in Fig. 7 we represent the ratio of electrons that cross the barrier from the GaAs to the AlGaAs over the total number of electrons that reach the heterojunction. The behavior explained before now becomes clear. RST begins to be significant for a biasing of 0.5 V, when the energy of the electrons is enough to jump over the barrier. Then RST increases not only because of the increasing energy of the electrons, but also because of the important occupation of the

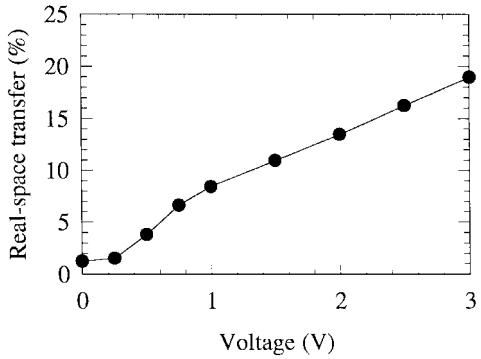

Fig. 7. Percentage of electrons surmounting the energy barrier over the total number of electrons arriving to the heterojunction.

higher valleys, where RST is easier. This result can explain the evolution of the current variance with the applied voltage, shown in Fig. 4. The appearance of RST and intervalley mechanisms (k-space transfers) give rise to fluctuations in the velocities of the carriers undergoing such kind of processes, and as a consequence the fluctuations of the current increase, leading to a higher current variance.

As the next step in our study, we have analyzed the time the electrons take to travel through the devices (transit time). In Fig. 8(a) the distribution of the transit times of the electrons arriving to the drain (coming from the source) is presented for both the u-HEMT and the u-MESFET, and in Fig. 8(b) the corresponding distribution of transit velocities (calculated by dividing the length of the device by the transit time of the carriers). It is observed how the transit time distribution in the u-MESFET spreads over longer times, which results in a wider distribution of transit velocities, mainly because of the presence of slow carriers (which also shifts the distribution to lower values of the velocity). If the time distribution were a $\delta(t_0)$, it would mean that all the electrons move with the same velocity ($\delta(v_0)$ as velocity distribution), leading to a current without any diffusion noise (the noise would be that associated to the fluctuations in the number of particles). The wider the transit velocity (or transit time) distribution is, the larger the fluctuations in the current are. So the connection between the results shown in Fig. 8 and the noise behavior of the devices is clear, and it can explain the lower value of the current variance of the u-HEMT (shown in Fig. 4). However, we must point out that the fluctuations of the current (and the variance) are not only associated to the carriers reaching the drain and coming from the source, but to all the carriers inside the device, some of which can return to the contact they entered from. The fluctuations of the carrier number can also be another source of noise. When we analyze the transit-time distribution we are dealing only with velocity fluctuations of the carriers crossing the device, which constitute the main contribution to the total current noise.

The transit-time distribution in the u-HEMT, together with the part of the time the electrons spend in each material are shown in Fig. 9 for different biasings. It can be observed how by increasing the biasing the confinement of electrons in the GaAs decreases, and the conduction of electrons is moved to the AlGaAs due to the appearance of RST's.

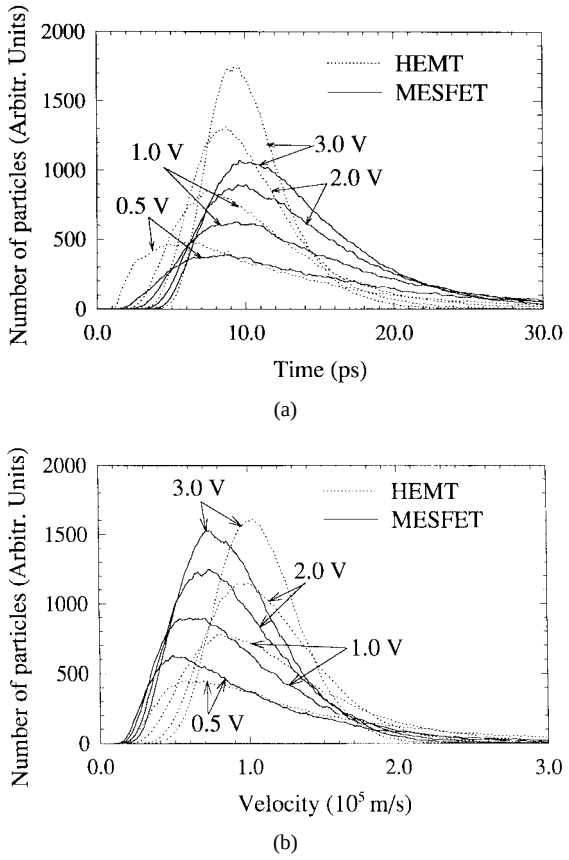

Fig. 8. (a) Transit time and (b) transit velocity distribution of the electrons arriving at the drain and coming from the source in the simulated u-HEMT and u-MESFET for different biasings.

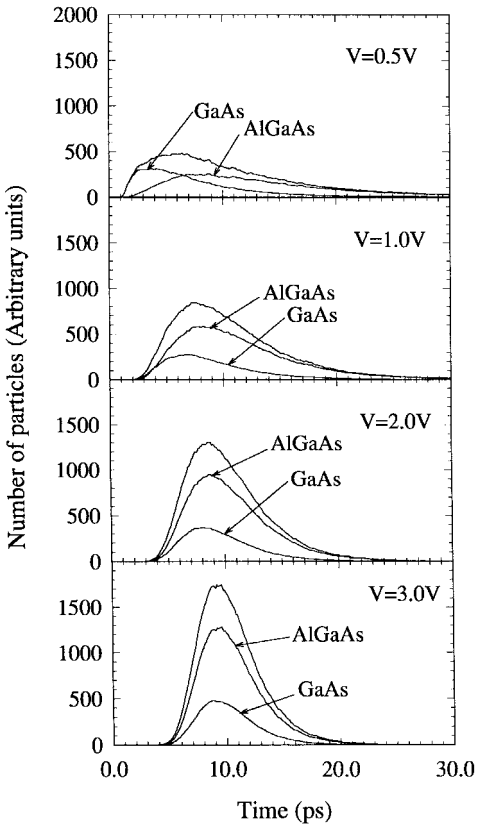

Fig. 9. Transit time distribution and part of the time spent by the electrons in the GaAs and AlGaAs layers in the simulated u-HEMT.

The carriers with low transit velocities present in the u-MESFET [Fig. 8(b)] are suppressed in the u-HEMT, thus producing a narrower distribution. The long time tail of the transit time distribution in both devices comes from carriers mainly present in the Γ valley (in the AlGaAs in the case of the u-HEMT). This means that these carriers are not under the action of a high electric field, since their effective mass is low and they would be easily accelerated. These low electric fields are found in the highly doped regions near the source and drain contacts of the devices (Fig. 6). The difference lies in the fact that in the u-HEMT the electric field penetrates deeper into the drain region, accelerating these slow electrons and thus diminishing considerably the long time tail of the distribution. In the case of the u-MESFET, when the applied voltage is increased the electric field in the drain region remains almost null, and therefore the slow part of the distribution does not decrease as much as it does in the u-HEMT. Moreover, when the biasing is sufficient for the beginning of RST, the number of fast electrons is also reduced, which also narrows the distribution in the u-HEMT. These fast electrons were strongly accelerated by the electric field while remaining in the Γ valley. RST processes decrease the velocity of the carriers, since the velocity is lower in AlGaAs than in GaAs due to: 1) the higher effective mass, 2) the more probable impurity scattering due to the higher doping, 3) the intervalley transfers appears more easily since the higher valleys are lower in energy, and 4) the important loss of energy the electrons suffer when a RST happens in the Γ valley. This effect is enhanced by the appearance of intervalley scatterings, in both AlGaAs and GaAs. The decrease in the velocity of the fast electrons in the u-MESFET distribution comes only from intervalley mechanisms, and therefore this effect is less pronounced.

At low fields in the u-HEMT, when the RST and intervalley mechanisms are not frequent, most of the current comes from electrons in the Γ valley flowing through the GaAs channel. If an electron moves inside the AlGaAs its velocity is much lower, because of the reasons given above. In Fig. 9, for a biasing of 0.5 V, this effect is clearly observed: two different distributions with quite different velocities appear, a faster one for GaAs and a slower one for AlGaAs. Therefore, under these conditions RST's imply an important change in the velocity of the carriers, leading to a widening of the time distribution by an enlargement of the long time tail. If the biasing increases, the electrons in both GaAs and AlGaAs suffer intervalley mechanisms, and their velocities become more similar. In Fig. 9 it is noticed how the difference between both distributions decreases with the biasing. If a RST mechanism occurs, the change in the velocity of the electron is not important and it does not affect the width of the distribution. In this way it can be explained the fact that the current variance increases when the RST begins, and why it saturates [Fig. 4] for high applied voltages even if the RST grows continuously [Fig. 7].

In Fig. 10 the average transit time and the average transit velocity of the electrons in both the u-HEMT and the u-MESFET are presented. It can be observed that when the

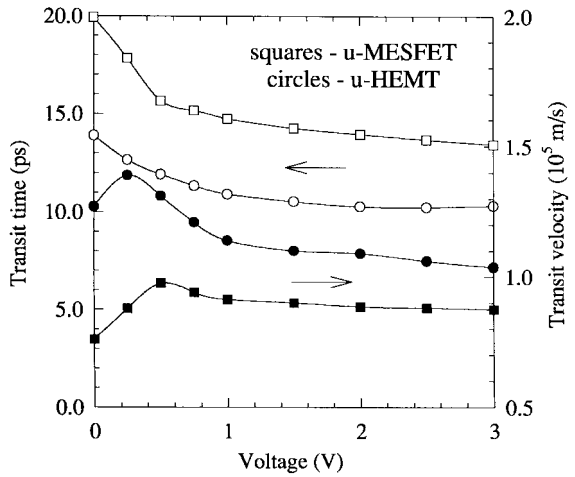

Fig. 10. Average transit time (open symbols) and average transit velocity (close symbols) of the electrons in the simulated u-HEMT (circles) and u-MESFET (squares) as a function of the applied voltage.

applied voltage increases the average transit time in the u-HEMT decreases even if the population of the GaAs is reduced, since the effect of the long-time-tail suppression is more significant. In the u-MESFET the behavior is similar, the acceleration of the slow electrons is stronger than the loss of velocity of the fast ones. In the case of the average transit velocity, $\langle v_t \rangle$, we observe a different behavior. The reason is that the slow carriers do not influence on $\langle v_t \rangle$ as much as they do on the average transit time, since the most weighted electrons in the transit velocity distribution are the fast ones. At low biasings the average transit velocity increases due to the growing electric field, which accelerates the electrons. But the beginning of RST and intervalley mechanisms reduces the number of fast electrons, and $\langle v_t \rangle$ decreases. Comparing the u-MESFET and the u-HEMT we can observe that the peak of $\langle v_t \rangle$ appears at a higher biasing for the u-MESFET. This is because of the effect of the RST, which appears at lower energies than intervalley mechanisms. Thus the velocity of the electrons of the u-HEMT is reduced at lower voltages (so displacing the $\langle v_t \rangle$ peak) than in the u-MESFET, where the reduction of the velocity comes only from the intervalley mechanisms. The most important fact is that the u-HEMT is more than 30% faster than the u-MESFET, reaching switch-on times near 10 ps, corresponding to an average transit velocity peak of 1.4 10^5 m/s (in the u-MESFET is only of about 10^5 m/s). Therefore, by studying the electron transit-time distribution it is possible to explain the faster behavior of the u-HEMT.

From the results for all the biasings we can conclude that the electrons traveling through the AlGaAs make the transit time become longer and the time distribution wider, so degrading both the speed and the noise behavior of the u-HEMT. Consequently, the confinement of the current in the GaAs channel must be improved to optimize the device performance.

V. Conclusion

We have performed a Monte-Carlo analysis of the velocity and noise performance of one GaAs/AlGaAs u-HEMT compared with those of one GaAs u-MESFET. The devices object of our study are ungated to reduce the number of noise parameters to be considered and to avoid experimental complications, and recessed to have an effect similar to that of a gate, so we get near the behavior of a conventional gated transistor. Firstly the Monte-Carlo modeling has been contrasted with experimental results of static characteristics and noise temperature, finding a very good agreement and so confirming the reliability of the simulation. The noise temperature has been found to be not completely appropriate for the comparison of the current noise behavior of a u-HEMT and a u-MESFET with the same level of current, because it includes the influence of the small signal parameters of the device, and so somewhat masking the noise performance. The variance of the current, which represents the total noise spectrum, makes easier the comparison of the noise behavior of the devices, showing the great difference (a factor 2) existing between them. The internal processes taking place inside of the u-HEMT, as RST and transverse domain formation, have been studied, and the connection between the beginning of RST and the increase of the noise has been demonstrated.

The transit time of electrons is an interesting magnitude to analyze the device performance because it provides information not only about the speed of the device, but also about the noise. The average transit time of the u-HEMT has been calculated and found to be near 10 ps (much shorter than in the u-MESFET, where it is about 14 ps). The distribution of the transit time is related to the velocity distribution and so to the current fluctuations. If carriers with very different velocities are present, the current they will produce will have strong fluctuations. This is the case of the u-MESFET, whose transit time and velocity distributions spread much more than in the u-HEMT.

References

[1] R. J. Nelson, "Long lifetime photoconductivity effect in n-type GaAlAs," *Appl. Phys. Lett.*, vol. 31, p. 351, 1977.
[2] D. V. Lang, R. A. Logan, and M. Jaros, "Trapping characteristics and a donor-complex (DX) model for the persistent photoconductivity trapping center in Te-doped $Al_xGa_{1-x}As$," *Phys. Rev. B*, p. 1015, 1979.
[3] A. Kastalsky and R. Kiehl, "On the low temperature degradation of AlGaAs/GaAs modulation-doped field effect transistors," *IEEE Trans. Electron Devices*, vol. ED-33, p. 414, 1986.
[4] C. Jacoboni and P. Lugli, *The Monte-Carlo Method for Semiconductor Device Simulation*. Vienna, Austria: Springer-Verlag, 1989.
[5] C. Jacoboni and L. Reggiani, "The Monte-Carlo method for the solution of charge transport in semiconductors with application to covalent materials," *Rev. Mod. Phys.*, vol. 55, p. 645, 1983.
[6] M. Tomizawa, A. Yoshii, and K. Yokoyama, "Modeling for an AlGaAs/GaAs heterostructure device using Monte-Carlo simulation," *IEEE Electron Device Lett.*, vol. EDL-6, p. 332, 1985.
[7] U. Ravaioli and D. Ferry, "MODFET ensemble Monte-Carlo model including the quasi-two-dimensional electron gas," *IEEE Trans. Electron Devices*, vol. ED-33, p. 677, 1986.
[8] D. H. Park, Y. Wang, and K. F. Brennan, "Ensemble Monte-Carlo simulation of a 0.35-μm pseudomorphic HEMT," *IEEE Electron Device Lett.*, vol. 10, p. 107, 1989.
[9] D. J. Widiger, K. Hess, and J. J. Coleman, "Two-dimensional numerical analysis of the high electron mobility transistor," *IEEE Electron Device Lett.*, vol. EDL-5, p. 266, 1984.
[10] D. J. Widiger, I. C. Kizilyalli, K. Hess, and J. J. Coleman, "Two-dimensional transient simulation of an idealized high electron mobility transistor," *IEEE Trans. Electron Devices*, vol. ED-32, p. 1092, 1985.
[11] K. Yokoyama and K. Hess, "Monte-Carlo study of electronic transport in $Al_xGa_{1-x}As$/GaAs single-well heterostructures," *Phys. Rev. B.*, vol. 33, p. 5595, 1986.

[12] K. F. Brennan and D. H. Park, "Theoretical comparison of electron real-space transfer in classical and quantum two-dimensional heterostructure systems," *J. Appl. Phys.*, vol. 65, p. 1156, 1989.
[13] J. Mateos, T. González, D. Pardo, P. Tadyszak, F. Danneville, and A. Cappy, "Numerical and experimental analysis of static characteristics and noise in ungated recessed MESFET structures," *Solid-State Electron.*, vol. 39, p. 1629, 1996.
[14] I. C. Kizilyalli, K. Hess, J. L. Larsson, and D. J. Widiger, "Scaling properties of high electron mobility transistors," *IEEE Trans. Electron Devices*, vol. ED-33, p. 1427, 1986.
[15] V. Mitin, V. Gruzinskis, E. Starikov, and P. Shiktorov, "Submillimeter wave generation and noise in InP diodes," *J. Appl. Phys.*, vol. 75, p. 935, 1994.
[16] F. Heliodore, M. Lefebvre, G. Salmer, and O. L. El-Sayed, "Two-dimensional simulation of submicrometer GaAs MESFET's: Surface effects and optimization of recessed gate structures," *IEEE Trans. Electron Devices*, vol. 35, p. 824, 1988.
[17] M. V. Fischetti and S. E. Laux, "Monte-Carlo analysis of electron transport in small semiconductor devices including band-structure and space-charge effects," *Phys. Rev. B*, vol. 38, p. 9721, 1988.
[18] T. González and D. Pardo, "Physical models of ohmic contact for Monte-Carlo device simulation," *Solid-State Electron.*, vol. 39, p. 555, 1996.
[19] J. Mateos, T. González, and D. Pardo, "Spatial extent of the correlation between local diffusion noise sources in GaAs," *J. Appl. Phys.*, vol. 77, p. 1564, 1995.
[20] T. González, J. E. Velázquez, P. M. Gutierrez, and D. Pardo, "Five valley model for the study of electron transport properties at very high electric fields in GaAs," *Semicond. Sci. Technol.*, vol. 6, p. 862, 1991.
[21] L. Pavesi and M. Guzzi, "Photoluminiscence of $Al_xGa_{1-x}As$ alloys," *J. Appl. Phys.*, vol. 75, p. 4779, 1994.
[22] I. C. Kizilyalli, M. Artaki, and A. Chandra, "Monte-Carlo study of $GaAs/Al_xGa_{1-x}As$ MODFET's: Effects of $GaAs/Al_xGa_{1-x}As$ composition," *IEEE Trans. Electron Devices*, vol. 38, p. 197, 1991.
[23] T. Wang and K. Hess, "Calculation of the electron velocity distribution in high electron mobility transistors using an ensemble Monte-Carlo method," *J. Appl. Phys.*, vol. 57, p. 5336, 1985.
[24] R. Sakamoto, K. Akai, and M. Inoue, "Real-space transfer and hot-electron transport properties in III-V semiconductor heterostructures," *IEEE Trans. Electron Devices*, vol. 36, p. 2344, 1989.
[25] K. F. Brennan, D. H. Park, K. Hess, and M. A. Littlejohn, "Theory of the velocity-field relation in AlGaAs," *J. Appl. Phys.*, vol. 63, p. 5004, 1988.
[26] M. O. Watanabe, J. Yoshida, M. Mashita, T. Nakanisi, and A. Hojo, "Band discontinuity for GaAs/AlGaAs heterojunction determined by C-V profiling technique," *J. Appl. Phys.*, vol. 57, p. 5340, 1985.
[27] G. U. Jensen, B. Lund, T. A. Fjeldly, and M. Shur, "Monte-Carlo simulation of short-channel heterostructure field-effect transistors," *IEEE Trans. Electron Devices*, vol. 38, p. 840, 1991.
[28] G. Dambrine, H. Happy, F. Danneville, and A. Cappy, "A new method for on wafer noise measurements," *IEEE Trans. Microwave Theory Tech.*, vol. 41, p. 375, 1993.
[29] L. Varani, L. Reggiani, T. Kuhn, T. González, and D. Pardo, "Microscopic simulation of electronic noise in semiconductor materials and devices," *IEEE Trans. Electron Devices*, vol. 41, p. 1916, 1994.
[30] Y. Awano, M. Kosugi, K. Kosemura, T. Mimura, and M. Abe, "Short-channel effects in subquarter-micrometer-gate HEMT's: Simulation and experiment," *IEEE Trans. Electron Devices*, vol. 36, p. 2260, 1989.

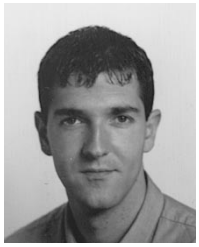

Javier Mateos was born in Salamanca, Spain, in 1970. He graduated from the University of Salamanca with a degree physics in 1993. He is currently pursuing the Ph.D. degree at the same university.

Since 1993, he has been working with the Electronics Group in the Department of Applied Physics, University of Salamanca, as a Grant Holder. In 1994, he worked for six months at the Institut d'Electronique et de Microelectronique du Nord (IEMN). In 1996, he became an Assistant Professor. His present research interest is the modeling of submicron heterojunction devices, focusing on the study of electronic noise.

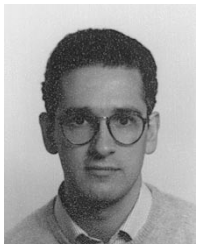

Tomás González was born in Salamanca, Spain, in 1967. He received the B.S. and Ph.D. degrees in physics from the University of Salamanca in 1990 and 1994, respectively.

Since 1991, he has been working with the Electronics Group in the Department of Applied Physics, University of Salamanca, with a grant from the Spanish Education Ministry. In 1996, he became Associate Professor. His main research activity is in the field of electronic transport in semiconductor materials and devices with special application to Monte-Carlo simulation of electronic noise.

Daniel Pardo was born in Valladolid, Spain, in 1946. He received the B.S. and Ph.D. degrees in physics from the University of Valladolid, Spain, in 1971 and 1975, respectively.

From 1971 to 1981, he was working in the Electronics Department, University of Valladolid, on the characterization of semiconductor materials and modeling of semiconductor devices. He was promoted to Associate Professor there in 1978. In 1981, he joined the Applied Physics Department, University of Salamanca, Salamanca, Spain, where he has been a Full Professor since 1983, and is Head of the Electronics Group. His current research interest is the Monte-Carlo simulation of semiconductor devices with special application to noise characterization.

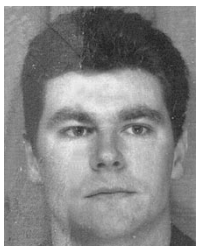

Patrick Tadyszak was born in Douai, France, on February 23, 1969. He received the M.Sc. degree from the University of Lille I, France, in 1992. He is currently pursuing the Ph.D. degree in the Institut d'Electronique et de Microelectronique du Nord (IEMN) at the same university.

In 1994, he worked in the Department of Physics, University of Modena, Italy. His main research interests are concerned with noise modeling and characterization techniques for application in the centimeter-wave range.

François Danneville was born in Ham, France, on March 16, 1964. He received the Ph.D. degree from the Centre Hyperfrequences et Semiconducteurs, University of Lille I, France, in 1991.

He is currently a Lecturer with the Institut d'Electronique et de Microelectronique du Nord (IEMN) at the University of Lille. His main research interests are concerned with noise modeling in field effect transistors under linear and nonlinear operation for application in the centimeter- and millimeter-wave ranges.

Alain Cappy was born in Chalons sur Marne, France, on January 25, 1954. In 1977, he joined the Centre Hyperfrequences et Semiconducteurs, University of Lille, France, where he received the Docteur en Sciences degree for his work on the modeling and the characterization of MESFET's and HEMT's in 1986.

He is now Professor of Electronics at the University of Lille. His main research interests are concerned with the modeling, realization, and characterization of low-noise devices for application in the centimeter- and millimeter-wave ranges.